Chapter 4 POSTER PRESENTATIONS

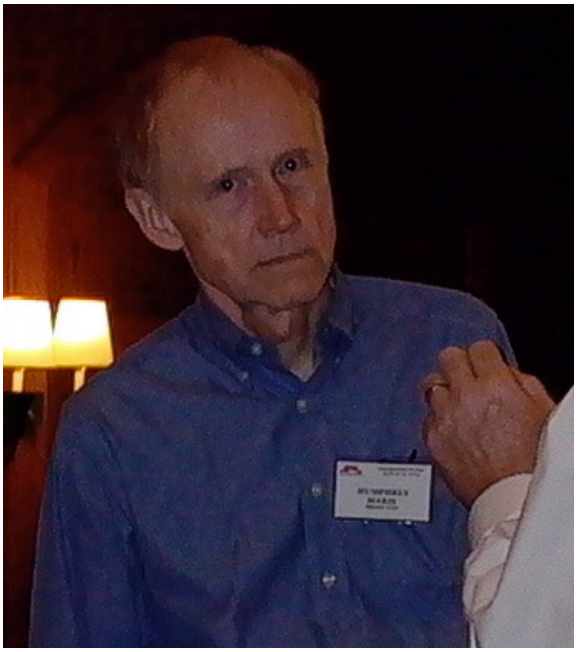


PETER
WEICHMAN

Radiation Detection and Monitoring in Space with Low-Temperature Bolometric Techniques

Stephen Boyd
University of New Mexico, Dept. of Physics and Astronomy
800 Yale Blvd NE
Albuquerque, NM 87131-1156

Low-temperature bolometric techniques present advantages and unique capabilities for radiation detection compared to standard detectors, because their detection physics is fundamentally different from that of standard detectors. Among these advantages are: direct sensitivity to energy deposition by all forms of radiation, including neutral particles; extremely low threshold for energy absorption; and a wide choice of absorber materials including materials with high neutron absorption. Near 0.3K, a space-capable detector of useful size should be able to achieve ~150 eV of energy resolution, a substantial improvement over solid-state detectors. In addition, the use of a neutron-detecting absorber in such a detector would constitute a uniquely capable and compact neutron spectrometer. Real-time onboard neutron spectrometry would be particularly valuable for space exploration missions because secondary neutrons from incident cosmic rays are a major source of radiation hazard for interplanetary missions, and the health effects of these neutrons are strongly energy-dependent. We review the case for using these new detectors in space exploration missions and report on our ongoing development work.

High-Resolution Displacement Sensor Using a SQUID Array Amplifier

Talso Chui, Konstantin Penanen, M. Barmatz
Jet Propulsion Laboratory, California Institute of Technology, CA 91109

Ho Jung Paik
Department of Physics, University of Maryland, College Park, MD 20742

Improvement in the measurement of displacement has profound implications for both exploration technologies and fundamental physics. For planetary exploration, the new SQUID-based capacitive displacement sensor will enable a more sensitive gravity gradiometer for mapping the interior of planets and moons. A new concept of a superfluid clock to be reported by Penanen and Chui at this workshop is also based on a high-resolution displacement sensor. Examples of high-impact physics projects that can benefit from a better displacement sensor are: detection of gravitational waves, test of the equivalence principle, search for the postulated "axion" particle, and test of the inverse square law of gravity. We describe the concept of a new displacement sensor that makes use of a recent development in the Superconducting Quantum Interference Device (SQUID) technology. The SQUID array amplifier, invented by Welty and Martinis (IEEE Trans. Appl. Superconductivity **3**, 2605, 1993), has about the same noise as a conventional SQUID; however, it can work at a much higher frequency of up to 5 MHz. We explain how the higher bandwidth can be translated into higher resolution using a bridge-balancing scheme that can simultaneously balance out both the carrier signal at the bridge output and the electrostatic force acting on the test mass.

The work described here was carried out at the Jet Propulsion Laboratory, California Institute of Technology, under a contract with the National Aeronautics and Space Administration.

Thermal and Quantum Mechanical Noise of a Superfluid Gyroscope

Talso Chui and Konstantin Penanen

Jet Propulsion Laboratory, California Institute of Technology
4800 Oak Grove Drive, Mail Stop 79-24
Pasadena, CA 91109

A potential application of a superfluid gyroscope is for real-time measurements of the small variations in the rotational speed of the Earth, the Moon, and Mars. Such rotational jitter, if not measured and corrected for, will be a limiting factor on the resolution potential of a GPS system. This limitation will prevent many automation concepts in navigation, construction, and biomedical examination from being realized. We present the calculation of thermal and quantum-mechanical phase noise across the Josephson junction of a superfluid gyroscope. This allows us to derive the fundamental limits on the performance of a superfluid gyroscope. We show that the fundamental limit on real-time GPS due to rotational jitter can be reduced to well below 1 millimeter/day. Other limitations and their potential mitigation will also be discussed.

The work described here was carried out at the Jet Propulsion Laboratory, California Institute of Technology, under a contract with the National Aeronautics and Space Administration.

Using the Moon and Mars as Giant Detectors for Strange Quark Nuggets

Talso Chui, Konstantin Penanen, Don Strayer, Bruce Banerdt
Jet Propulsion Laboratory, California Institute of Technology
Pasadena, CA 91109

Vigdor Tepliz
Goddard Space Flight Center
Greenbelt, MD 20771

Eugene Herrin
Southern Methodist University
Dallas, TX 75205

On the Earth, the detectability of small seismic signals is limited by pervasive seismic background noise, caused primarily by interactions of the atmosphere and oceans with the solid surface. Mars, with a very thin atmosphere and no ocean is expected to have a noise level at least an order of magnitude lower than the Earth, and the airless Moon is even quieter still. These pristine low-vibration environments are ideal for searching for nuggets of "strange quark matter." Strange quark matter was postulated by Edward Witten [Phys. Rev. D30, 272, 1984] as the lowest possible energy state of matter. It would be made of up, down, and strange quarks, instead of protons and neutrons made only of up and down quarks. It would have nuclear densities, and hence be difficult to detect. Micron-sized nuggets would weigh in the ton range. As suggested by de Rujula and Glashow [Nature 312 (5996): 734, 1984], a massive strange quark nugget can generate a trail of seismic waves, as it traverses a celestial body. We discuss the mission concept for deploying a network of sensitive seismometers on Mars and on the Moon for such a search.

The work described here was carried out in part at the Jet Propulsion Laboratory, California Institute of Technology under a contract with the National Aeronautics and Space Administration.

A Robust, Fast, and Deterministic Spike-reduction Algorithm for Autonomous Real-time Control

Dmitri A. Sergatskov, Qunzhang Li, and R. V. Duncan
Physics Department, University of New Mexico
800 Yale Blvd NE
Albuquerque, NM 87123

We consider the problem of measuring slowly-changing data in the presence of both white noise and sudden, short noise spikes. Such data are similar to those obtained in high resolution thermal experiments on earth orbit, where the thermometers are often struck and suddenly heated by charged particles. This problem is relevant to the development of control algorithms for the DYNAMX and CQ experiments. The previously flown low-temperature experiments LPE and CHeX solved this problem by using iterative re-weighting linear-fit methods. The performance of this procedure depends strongly on the characteristics of the input data, and there are known specific cases when the algorithm will not converge. This complicates the design of autonomous real-time systems where such a spike removal procedure is part of a control sequence.

We report on a new algorithm that is robust, with a fixed worst-case execution time. This new algorithm performs significantly faster than the CHeX algorithm in tests using both simulated and actual CHeX data.

Pulsed Electron Spin Resonance Spectrometer for Impurity-Helium Solids

David M. Lee
Cornell University Physics Dept.
Ithaca, NY 14853

A pulsed electron spin resonance (ESR) spectrometer, now under construction, is described. A TE-011 resonant cavity with a quality factor Q of approximately 700 has been designed and constructed. The low Q provides short cavity ring-down times. This instrument will be used to observe free induction decay and spin echoes. A search will be made for exchange narrowing in concentrated impurity-helium solids that would be manifested by at least part of the sample showing an anomalously long free-induction-decay tail. Exotic "solid echoes" will be used to explore the role of dipolar interactions in dilute free radical samples. An attempt will be made to study spin diffusion transport with the 90-180 echo technique in dilute free radical samples.

Demonstration of an Ultra-Stable Cryogenic Platform with 25 pK/root-Hz Stability

Colin J. Green(1), Dmitri A. Sergatskov(1), and R. V. Duncan(1,2)
1: The University of New Mexico, 2: California Institute of Technology

Existing paramagnetic susceptibility thermometers used in fundamental physics experiments near 2.2 K are capable of measuring temperature changes with a precision of about 100 pK in a one-hertz measurement bandwidth, with a demonstrated drift stability of about a nK per day. Commercial electrical heater controllers are only able to control power dissipation to a precision of about ten parts per million (ppm), with an open loop drift of about 50 ppm per day. We have developed an ultra-stable temperature platform with a demonstrated noise of 25 pK in a one-hertz bandwidth, and we have identified the physical source of this residual noise. We used an array of RF-biased Josephson junctions to precisely control the electrical power dissipation in a heater resistor mounted on this thermally isolated cryogenic platform to well beyond our ability to measure, which we estimate is stable to better than a part in 10^{12}. This Josephson heater controller may be used in a new synchronous demodulation circuit to maintain absolute temperature stability of the stage to about the same level as the demonstrated noise, provided that the ^{4}He superfluid transition temperature is fundamentally stable at this level. This work may provide a blackbody temperature reference for use in space radiometry applications that is considerably more stable than the temperature of the cosmic background radiation itself. This new technology may enable critical heat capacity measurements in ^{4}He within a weightless laboratory to a reduced temperature of about 10^{-11}, where the critical fluctuation lengths would be about a cm, and the fluctuation rates would be measurable within the bandwidth of the thermometry.

This work has been funded by the Fundamental Physics Discipline of the Microgravity Science Office of NASA, and was supported by a no-cost equipment loan from Sandia National Laboratories.

Measurements of thermal conductivity of superfluid helium near its transition temperature T_λ in a 2D confinement

Sergei Jerebets
NASA Jet Propulsion Laboratory, California Institute of Technology
4800 Oak Grove Drive, Pasadena, CA 91109

We report our recent experiments on thermal conductivity measurementsof superfluid ^{4}He near its phase transition in a two-dimensional (2D) confinement under saturated vapor pressure. A 2D confinement is created by 2-mm- and 1-mm-thick glass capillary plates, consisting of densely populated parallel microchannels with cross-sections of 5 x 50 and 1 x 10 microns, correspondingly. A heat current ($2 < Q < 400$ nW/cm^2) was applied along the channels' long direction. High-resolution measurements were provided by DC SQUID-based high-resolution paramagnetic salt thermometers (HRTs) with a nanokelvin resolution. We might find that thermal conductivity of confined helium is finite at the bulk superfluid transition temperature. Our 2D results will be compared with those in a bulk and 1D confinement.

The work described here was carried out at the Jet Propulsion Laboratory, California Institute of Technology, under a contract with the National Aeronautics and Space Administration.

New Precision-Feedback Controls for Low-Temperature Experiments

Jinyang Liu, Dmitri A. Sergatskov, and R. V. Duncan
University of New Mexico
800 Yale Blvd NE
Albuquerque, NM 87123

High-precision, low-temperature experiments usually consist of few thermal links. In first approximation, each stage can be represented by a large thermal mass connected to the other stages through weak thermal links. This model works especially well for experiments with superfluid helium near the lambda point, where the heat capacity of the helium sample is extraordinary large. The characteristic time constant of such a stage can be of the order of 100 to 100,000 seconds, which significantly exceeds all other characteristic times within the stage. We consider the problem of temperature control of such a system and devise control schemes that improve upon traditional proportional-integral-derivative (PID) methods. We show that a proportional-integral/proportional (PI/P) controller has a better ramp tracking and step response, and that the use of a Kalman filter for the input signal significantly decreases the noise injected from the feedback loop.

Entangled atomic clock

D. Matsukevich, A. Kuzmich,
S. Jenkins, and T.A.B. Kennedy

School of Physics,
Georgia Tech, Atlanta

Entangled states

$$\left.\begin{array}{l} |\uparrow\rangle \otimes |\uparrow\rangle \\ |\downarrow\rangle \otimes |\downarrow\rangle \end{array}\right\}$$ product states

$$\frac{1}{\sqrt{2}}\left(|\uparrow\rangle \otimes |\uparrow\rangle + |\downarrow\rangle \otimes |\downarrow\rangle\right)$$ entangled state

Schrodinger (1935): “I would not call (entanglement) one, but rather the characteristic trait of quantum mechanics, the one that enforces its entire departure from classical lines of thought.”

Continuous quantum variables

From large spins to continuous variables

$$\left[J_y, J_z \right] = iJ_x$$

however for large, well defined mean angular momenta

$J_x \cong \langle J_x \rangle = J = N/2$ for N spin ½ particles

$$\therefore \left[\frac{J_y}{\sqrt{J}}, \frac{J_z}{\sqrt{J}} \right] = i \frac{J_x}{J} \qquad i \Leftrightarrow \left[X, P \right] = i$$

∴ continuous CNOT is realised by two large spins

$$U = e^{-iX_1 X_2} = e^{-iS_z F_z / \sqrt{SF}}$$

Atoms as a continuous quantum variable system

•single atomic spin

$$f_x = \frac{1}{2}\left(|1\rangle\langle 2| + |2\rangle\langle 1|\right)$$

$$f_y = \frac{1}{2i}\left(|1\rangle\langle 2| - |2\rangle\langle 1|\right)$$

$$f_z = \frac{1}{2}\left(|1\rangle\langle 1| - |2\rangle\langle 2|\right)$$

$$\mathbf{F} = \sum_{\mathbf{k}} \mathbf{f}^{\mathbf{k}}$$

For $< \hat{F}_x > \cong F$

$$[\hat{F}_y / \sqrt{F}, \hat{F}_z / \sqrt{F}] \cong i \Leftrightarrow [\hat{X}, \hat{P}] \cong i$$

Bloch vector

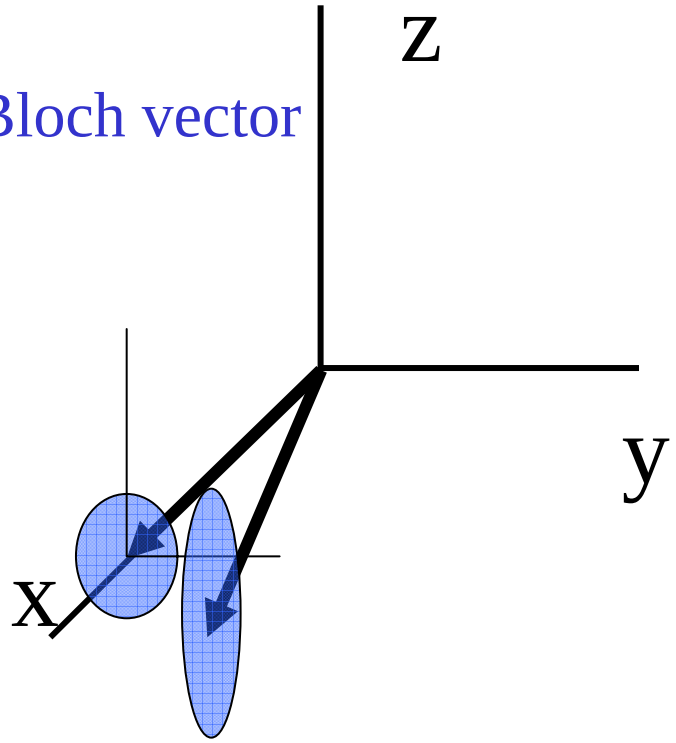

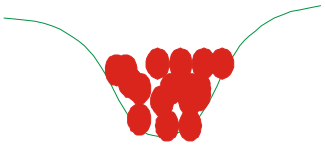

cold trapped atoms

MOT or FORT

Light as a continuous quantum variables system

- Stokes parameters

$$\hat{S}_{y,\mathrm{in}} = -\tfrac{i}{2}\int_0^T \mathrm{d}t(\hat{a}_1^\dagger(0,t)\hat{a}_2(0,t) - \hat{a}_1^\dagger(0,t)\hat{a}_2(0,t))$$
$$\hat{S}_{x,\mathrm{in}} = \tfrac{1}{2}\int_0^T \mathrm{d}t(\hat{a}_1^\dagger(0,t)\hat{a}_2(0,t) + \hat{a}_1^\dagger(0,t)\hat{a}_2(0,t))$$
$$\hat{S}_{z,\mathrm{in}} = \tfrac{1}{2}\int_0^T \mathrm{d}t(\hat{a}_1^\dagger(0,t)\hat{a}_1(0,t) - \hat{a}_2^\dagger(0,t)\hat{a}_2(0,t))$$

For $< \hat{S}_x > \cong S$

$$[\hat{S}_y / \sqrt{S}, \hat{S}_z / \sqrt{S}] \cong i,$$

$$[\hat{X}, \hat{P}] \cong i$$

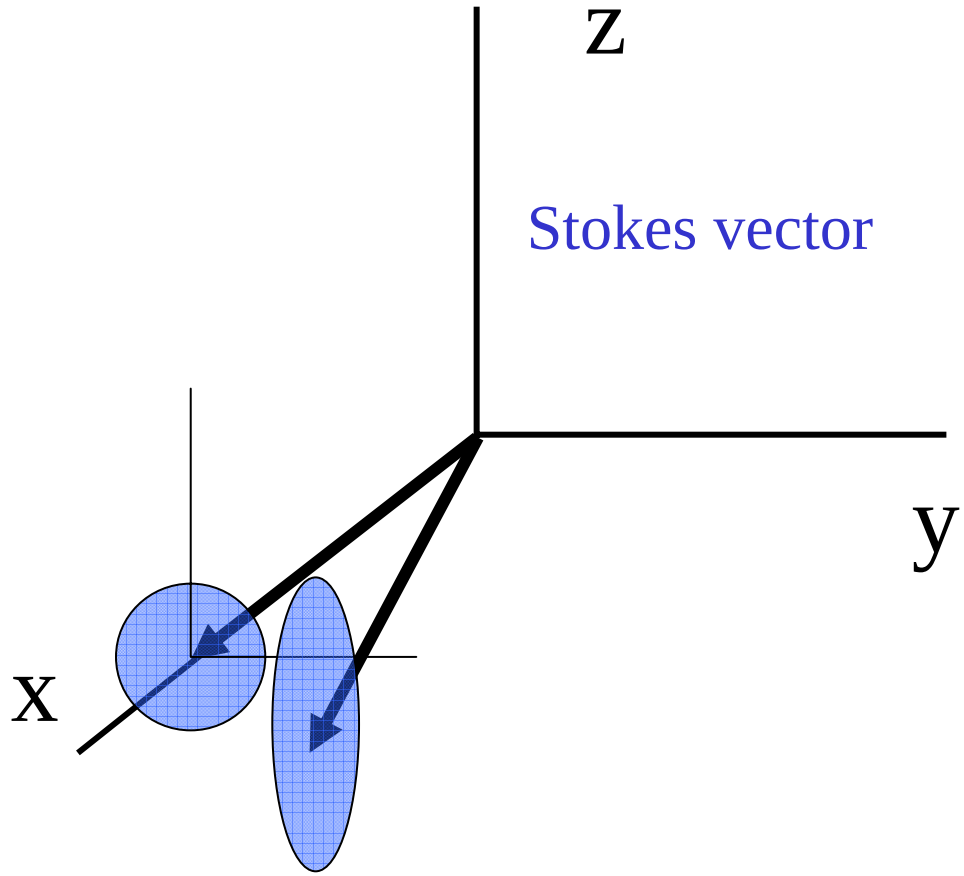

Off-resonant electric dipole interaction

$$\hat{H}_{\text{int}} = -\hat{\mathbf{D}}\ \hat{\mathbf{E}}$$

$$= \hbar\Omega \underbrace{\sum_{k=1}^{N} f_z^k}_{\hat{F}_z} \underbrace{\sum_{i=1}^{n} \hat{s}_z^i}_{\hat{S}_z}$$

Atom number

Photon number

QND measurement interpretation:

Measure observable conjugate to $\hat{S}_z$, e.g., $\hat{S}_y$

then one obtains information about $\hat{F}_z$ without disturbance (back action)

Spin Squeezing via QND interaction

A. Kuzmich, N. P. Bigelow, and L. Mandel, *Europhysics Letters*, **42**, 481 (1998).

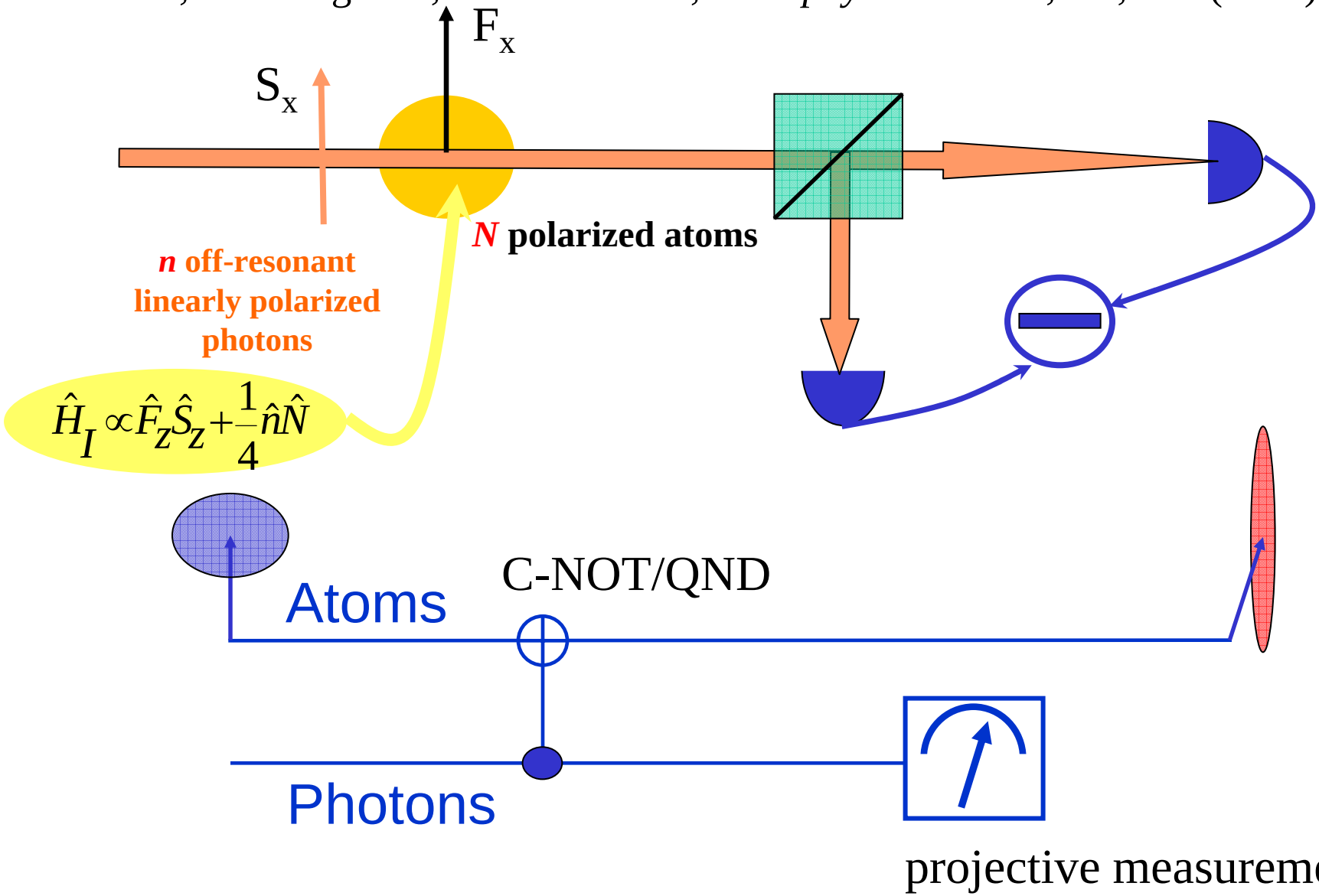

Clock transition

Kuzmich, GaTech

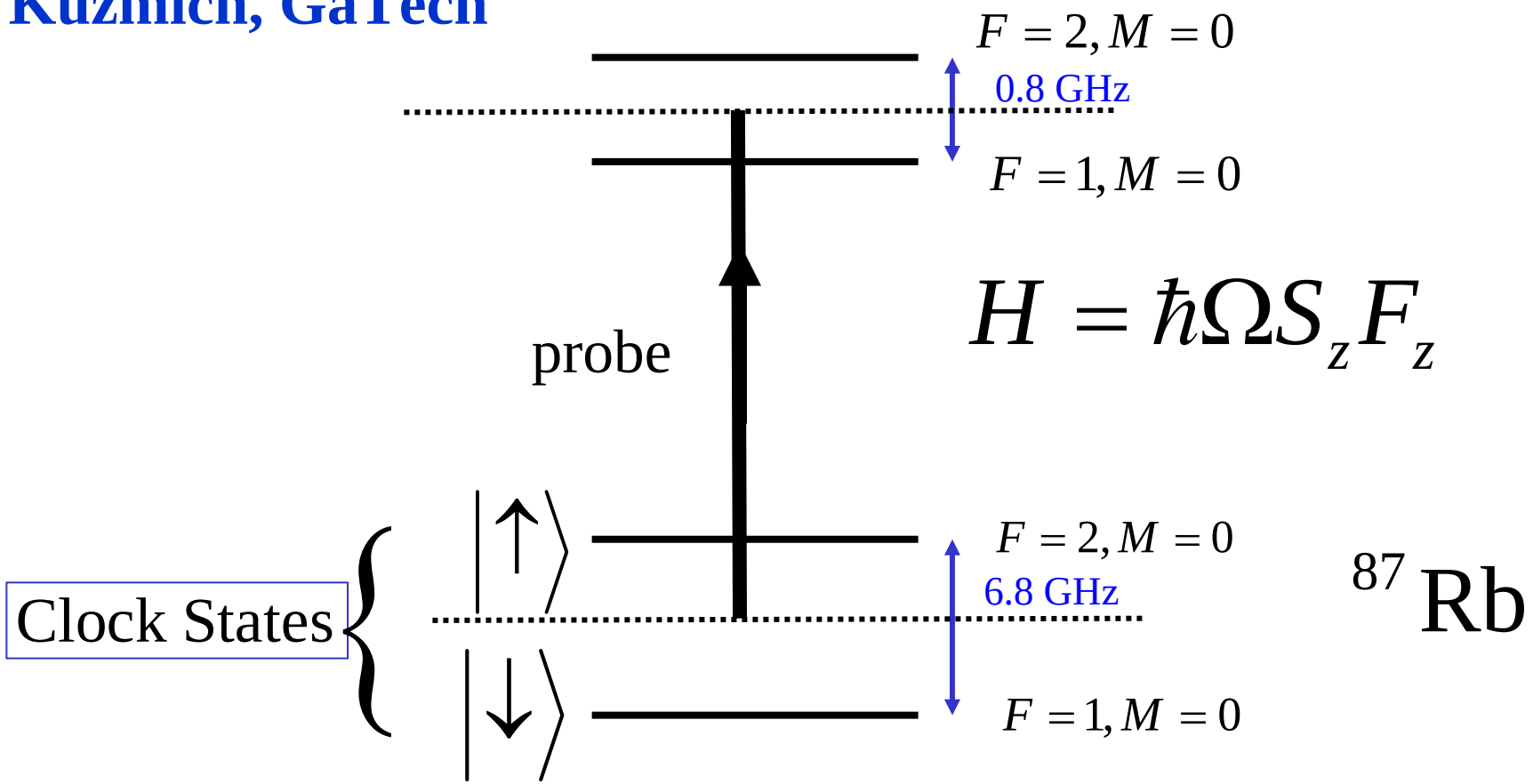

Atom-light continuous controlled-NOT gate

A. Kuzmich, N. P. Bigelow, and L. Mandel, *Europhysics Letters*, **42**, 481 (1998).

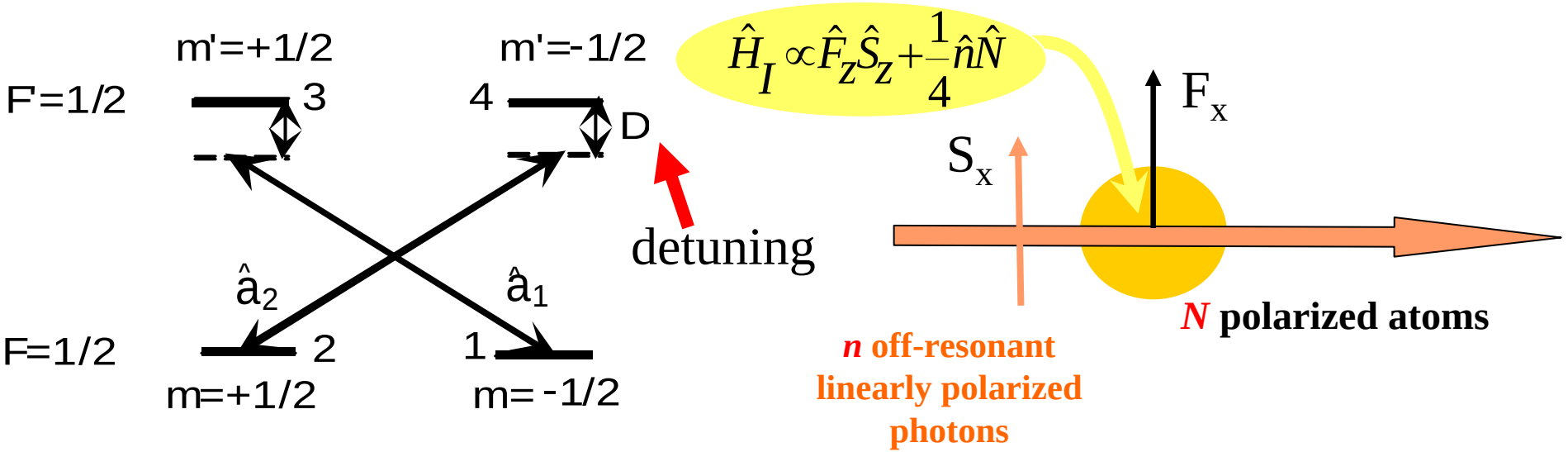

- Heisenberg picture dynamics

light: $\hat{S}_y^{out} = \hat{S}_y^{in} + a\hat{F}_z^{in}$

$\hat{S}_z^{out} = \hat{S}_z^{in}$

atoms: $\hat{F}_y^{out} = \hat{F}_y^{in} + a\hat{S}_z^{in}$

$\hat{F}_z^{out} = \hat{F}_z^{in}$

Don't need strong single photon-single atom coupling

Problem:
when atoms couple inhomogeneously to the laser field

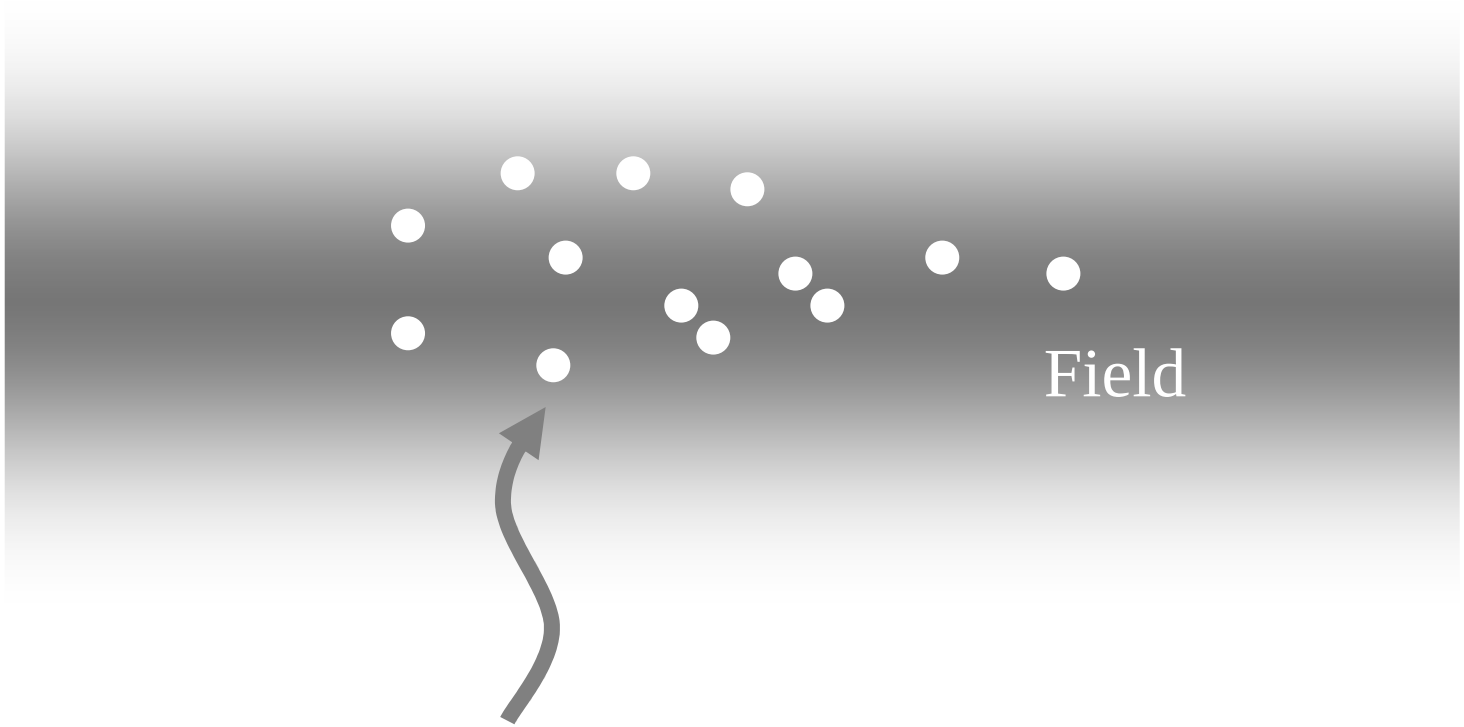

atom k coupling constant g_k

Experimental constraint: running waves with broad waist

Cavity QED- standing waves

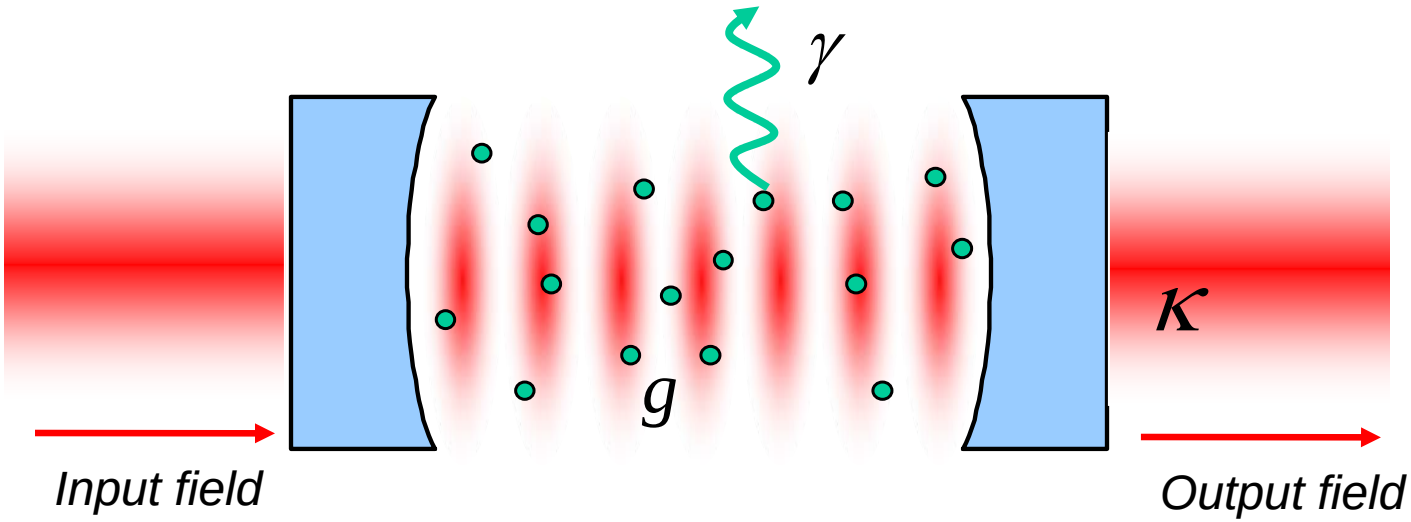

Off-resonant photon - atom ensemble interaction

$$\hat{H} = \hbar\Omega \sum_{i=1,k=1}^{n,N} g_k \hat{s}_z^i \hat{f}_z^k = \hbar\Omega \hat{S}_z \tilde{F}_z$$

inhomogeneous coupling

$$\hat{\mathbf{S}} = \sum_{i=1}^{n} \hat{\mathbf{s}}^i$$

Photon spin (single-mode)

$$\tilde{\mathbf{F}} = \sum_{k=1}^{N} g_k \hat{\mathbf{f}}^k$$

NOT atomic spin, unless $g_k = 1 \quad \forall k$

Photon spin $\hat{S}_z$ is NOT correlated to

$$\hat{F}_z = \sum_{k=1}^{N} \hat{f}_z^k$$

angular momentum

but, to

$$\tilde{F}_z = \sum_{k=1}^{N} g_k \hat{f}_z^k$$

random variable

Metrology-measuring small angles

Interferometer rotates spin

$$F_z^{out}(\phi) = e^{-iF_y\phi} F_z e^{iF_y\phi} \qquad F_z + \phi F_x$$

sensitivity

$$\delta\phi = \frac{\sqrt{\left\langle F_z^{out\ 2}(\phi = 0)\right\rangle}}{\left\langle \frac{dF_z^{out}}{d\phi}(\phi = 0)\right\rangle} = \frac{\sqrt{N}}{N} = \frac{1}{\sqrt{N}}$$

Projection noise

Heisenberg limit

$$\boxed{\delta\phi = \frac{1}{N}}$$

How ? spin squeezing of atoms (Wineland et al 1992,1994)

Projection Noise

Unavoidable fluctuations in the components orthogonal to the mean vector

$$\left[J_y, J_z \right] = iJ_x$$

$$\Delta J_y \Delta J_z \geq \frac{1}{2} \left| \left\langle J_x \right\rangle \right|$$

Clock accuracy limited by projection noise, e.g., H.Marion et al PRL 90, 150801 (2003)

Rotation angle measurement

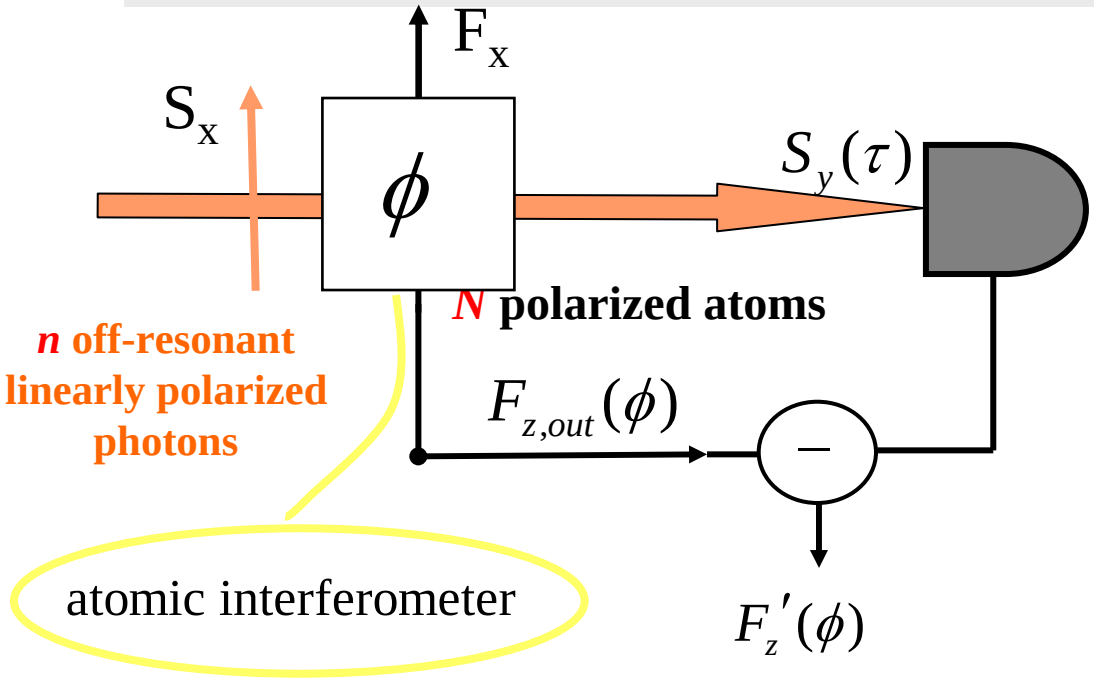

$2S_y(\tau)/(n\chi)$ $\quad \tilde{F}_z + 2S_y/(n\chi)$

$$F_{z,out} = F_z - \phi(\cdots\cdots)$$

$$F_z' \equiv F_{z,out} - 2S_y(\tau)/(n\chi)$$

Rotation angle measurement ctd.

Rotation angle sensitivity: $\delta\phi = \dfrac{\sqrt{\left\langle F_z'^{\,2}(\phi=0)\right\rangle}}{\left|\left\langle \dfrac{dF_z'}{d\phi}\right\rangle\right|_{\phi=0}}$

$$F_z'(\phi=0) = -\frac{2S_y}{n\chi} + \left(F_z - \tilde{F}_z\right) \qquad N \text{ dependent}$$

$$\left.\frac{dF_z'}{d\phi}\right|_{\phi=0} = -\sum_{k=1}^{N}\left(\cos(g_k\chi S_z)\, f^k{}_x - \sin(g_k\chi S_z)\, f^k{}_y\right) \qquad N$$

$$\chi \equiv \Omega\tau$$

A.Kuzmich and TABK, PRL 04

At optimum operating point

$$\delta\phi = \sqrt{\left[1 + N g_{rms}^2\right]\left[1 + g_{rms}^2\right]}\,\frac{e^{1/2\left[1+g_{rms}^2\right]}}{N} \rightarrow \frac{1}{\sqrt{N}}$$

Unless $g_{rms}^2 << \frac{1}{N}$ **we will not achieve Heisenberg scaling**

Optimum in absence of inhomogeneous broadening

$$\delta\phi_{\min} = \frac{\sqrt{e}}{N}$$

Elimination of inhomogeneous broadening

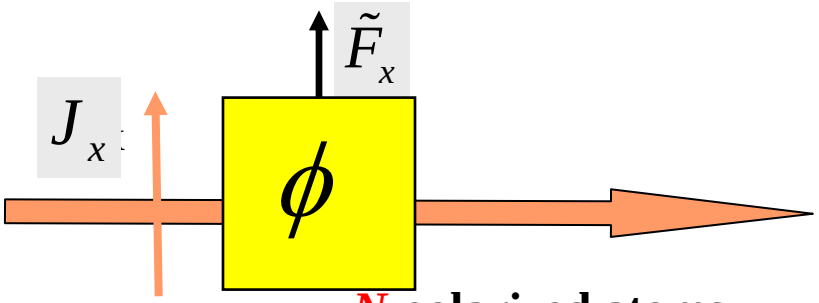

N **polarized atoms**

n **off-resonant linearly polarized photons**

$$A(\phi) = J_y(\tau) - S_y(\tau)$$

$$\left.\begin{aligned} \Delta A^2(\phi = 0) &= \Delta S_y^2 + \Delta J_y^2 \\ \left\langle \frac{dA(\phi)}{d\phi} \right\rangle_{\phi=0} &= \langle J_x \rangle \langle \tilde{F}_x(\tau) \rangle \cdot N \end{aligned}\right\} \quad \delta\phi_{\min} = \frac{\sqrt{2e}}{N}$$

Quantum Entanglement & Correlation of Bose Condensed Atoms

Li You
School of Physics
Georgia Tech
Atlanta, GA 30332

Abstract

At the frontier of atomic quantum gas research, a substantial topic of current interest is the creation of quantum correlated states of condensed atoms for several potential applications ranging from quantum computation to high precision quantum limited atom interferometry. In this study, we report our recent investigations of the generation and detection of quantum correlated states of Bose condensed atoms.
We have focused our efforts on two particular types of states that display inseparable quantum correlations: spin squeezed states and maximally entangled states.
We will present several protocols that can be implemented in laboratories of atomic quantum gases and provide explicit estimates for parameters and conditions relevant to their technological applications.

Quantum Entanglement & Correlation of Bose Condensed Atoms

Li You, *School of Physics, Georgia Tech, Atlanta, GA 30332*

$H = uS_x^2,$ Molmer and Sorensen, PRL **82**, 1835 (1999)

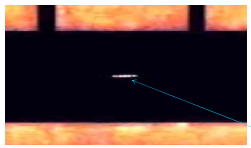

D. J. Wineland, and C. I. Monroe *et. al*, NATURE **404**, 256 (2000)

five $^9Be^+$ ions in linear trap

Creating maximally entangled atomic states in a condensate

$$|\text{N-GHZ}\rangle = \frac{1}{\sqrt{2}}\left(|\uparrow,\uparrow,\uparrow,\cdots\rangle + |\downarrow,\downarrow,\downarrow,\cdots\rangle\right)$$

L. You, Phys. Rev. Lett. **90**, 030402 (2003)

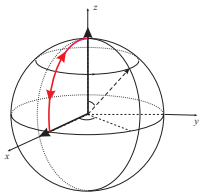

Two mode condensate $H = uS_z^2$ can be rotated into the x-direction with single atom Raman coupling $H = \Omega J_y$

Step 3 Step 1

$$U(t) \approx e^{i\frac{\pi}{2}S_y} e^{-iuS_z^2 t/\hbar} e^{-i\frac{\pi}{2}S_y} = e^{-iuS_x^2 t/\hbar}$$

Step 2

$$|\Omega| \gg |u|N$$

$$\langle \text{N-GHZ}|\rho_{N-particle}|\text{N-GHZ}\rangle > \frac{1}{2}$$

B. Zeng, D. L. Zhou, P. Zhang, Z. Xu, and L. You, PRA **68**, 042316 (2003).

Quantum Zeno subspaces in a spin-1 condensate

P. Facchi and S. Pascazio, Phys. Rev. Lett. **89**, 080401 (2002).

$H_K = H + K \bullet H_{\text{measurement}}$

FIG. 1 (color online). The Hilbert space of the system: an effective superselection rule appears as the coupling K to the apparatus is increased.

Optimal spin squeezing of condensed atoms

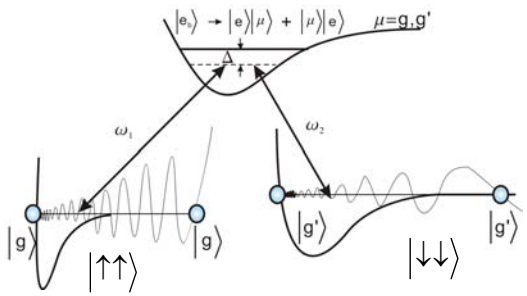

Kristian Helmerson and L. You, PRL. **87**, 170402 (2001).

M. Zhang and L. You, PRL, **91**, 230404 (2003)

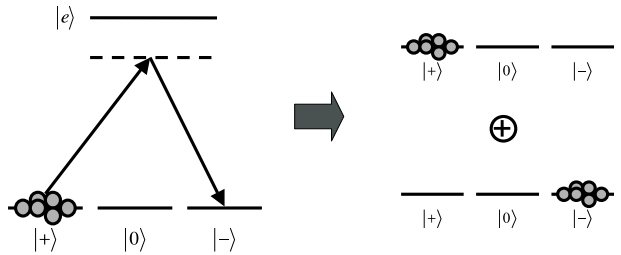

$$S^2 = 4T_3^2 + \frac{1}{2}\left(N-\varepsilon_+\right)\left(N-\varepsilon_-\right) - 2\left(Y-Y_0\right)^2 + G_Y$$

Gell-Mann decomposition

$$T_+ = a_+^\dagger a_-; \quad T_3 = \left(N_+ - N_-\right)/2$$
$$V_+ = a_+^\dagger a_0; \quad V_3 = \left(N_+ - N_0\right)/2$$
$$U_+ = a_-^\dagger a_0; \quad U_3 = \left(N_- - N_0\right)/2$$
$$Y = \left(N_+ + N_- - 2N_0\right)/3$$

$$G_Y = 2\left(V_+U_+ + h.c.\right)$$

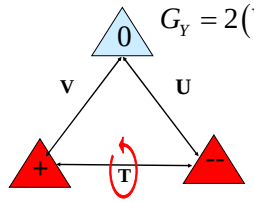

O. Mustecapliu, M. Zhang, and L. You, PRA **66**, 033611 (2002).

atomic excited state molecular excited state

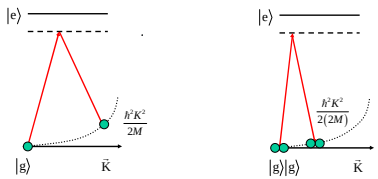

$$\frac{\hbar}{2}\Omega_R\left[\sigma_+^{(i)} \otimes \sigma_+^{(j)} + \sigma_-^{(i)} \otimes \sigma_-^{(j)}\right]$$

For every pair of atoms: absorption of one photon emission of one photon

Laser Ranging to the Moon, Mars and Beyond

Slava G. Turyshev, James G. Williams, Michael Shao
Jet Propulsion Laboratory, California Institute of Technology
4800 Oak Grove Drive, Pasadena, CA 91109

Kenneth L. Nordtvedt, Jr.
Northwest Analysis, 118 Sourdough Ridge Rd.
Bozeman MT 59715 USA

Thomas W. Murphy, Jr.
Physics Department, University of California, San Diego
9500 Gilman Dr., La Jolla, CA 92093

Current and future optical technologies will aid exploration of the Moon and Mars while advancing fundamental physics research in the solar system. Technologies and possible improvements in the laser-enabled tests of various physical phenomena are considered along with a space architecture that could be a cornerstone for robotic and human exploration in the solar system. In particular, accurate ranging to the Moon and Mars would not only lead to construction of a new space communication infrastructure enabling improved navigational accuracy, but would provide a significant improvement in several tests of gravitational theory: the equivalence principle, geodetic precession, PPN parameters beta and gamma, and the constancy of the gravitational constant G. Other tests would become possible with an optical architecture that would allow proceeding from cm to mm to sub-mm range accuracies. Looking to future exploration, what characteristics are desired for the next generation of ranging devices, what is the optimal architecture that would benefit both space exploration and fundamental physics, and what fundamental questions can be investigated?

The work described here was carried out at the Jet Propulsion Laboratory, California Institute of Technology under a contract with the National Aeronautics and Space Administration.

Critical point of oxygen with gravity cancellation

John Lipa
Stanford University, Physics Department
Stanford, CA 94305

We report the status of an experiment to reduce the effects of gravity at the critical point by using magnetic levitation. Measurements of the compressibility along isochores and the coexistence curve shape have been made. Future directions will also be described.

The Legacy of the Low Temperature Microgravity Physics Facility

Melora Larson, John Pensinger, Feng-Chuan Liu, Donald Langford, Inseob Hahn,
and G. John Dick
Jet Propulsion Laboratory, California Institute of Technology,
Pasadena, CA 91109

The Jet Propulsion Laboratory (JPL) has been building the Low Temperature Microgravity Physics Facility (LTMPF) as a multi-user research facility for the International Space Station. Because of the recent Presidential Exploration Initiative placed on NASA, NASA has informally told JPL to phase out the development of the LTMPF, assuming a suspension of funding at the end of fiscal year 2004. Over the last five years of development of the Facility, a tremendous legacy of both scientific and technical progress has been made, and a significant amount of flight hardware has been built. During these last few months of remaining funding, the LTMPF plans on finishing some remaining development efforts, archiving the hardware (flight and engineering models), software, and capturing the knowledge generated for possible future missions. These possible future missions could include gravitational or relativistic physics experiments (around the Earth or the Moon), charged particle physics experiments away from the Earth, possible other fundamental physics experiments in a Code U-developed free flyer orbiting the Earth, or even gravitational mapping experiments around the Moon or possibly Mars. LTMPF-developed technologies that are likely to have substantial impact on such future missions include SQUID magnetometers and thermometers, ultra-high-performance cryogenics, and high-Q superconducting resonators.

The work described here was carried out at the Jet Propulsion Laboratory, California Institute of Technology under a contract with the National Aeronautics and Space Administration.

Coalescence of Liquid Drops

Humphrey Maris
Brown University
Providence, RI 02912

When two liquid drops come into contact, driven by the surface tension, the neck connecting them will grow from a singular point. Recently, we studied such phenomena by measuring the neck size as a function of time. The speed with which the neck grows is determined by the surface tension and the viscosity of the liquid, and the size of the original drops. It takes less than 1 ms for two water drops of 1 cm in diameter to merge into one. The details of the coalescence process are hard to observe on this time scale. To study the details of coalescence, we have made measurements with silicone oil of high viscosity. To sustain a liquid globe of a size 10 cm in diameter, we built a Plateau tank. The silicone oil globes were immersed inside a second liquid with the same density to reduce the effect of the gravity.

In our study, we used three silicone oils with viscosity of 10, 100 and 1000 poise respectively, and two different drop sizes of 1 and 10 cm in diameter. Theory suggests that at the very initial stage of the coalescence the neck size r_n should change as a function of time following a certain relation relating r_n to the radius of the drops and to the viscosity and surface tension. In our experiment, we did observe that r_n scales with the time constant thus defined. However, our preliminary results indicate that r_n changes with time linearly for some circumstances.

Presentations of new results from Fundamental Physics research

Warren Nagourney
University of Washington
Seattle, WA

An optical frequency standard based upon a single, laser-cooled indium ion is shown to have a potential absolute inaccuracy of one part in 10^{18}. The current progress in constructing such a standard at the University of Washington will be presented. In addition, work is beginning on an optical frequency standard employing neutral ytterbium atoms trapped at the anti-nodes of an optical lattice. It will be shown that this approach can produce a standard with the extremely small systematic errors of single ions combined with a much greater signal-to-noise ratio due to the large number of atoms being interrogated. The current progress in ytterbium trapping will be presented together with the strategy we have chosen to construct an ytterbium frequency standard.

Spatial distribution of competing ions around DNA in solution

Lois Pollack
Cornell University
Applied & Engineering Physics
Ithaca, NY 14853

The competition of charged ions for proximity to negatively charged DNA has been studied with resonant x-ray scattering. The measured scattering profiles are in good agreement with calculations based on solutions of the Poisson-Boltzmann equation. These experiments aid in our understanding of the fundamental electrostatics of biological molecules.

Search for Lorentz violation using K-^{3}He co-magnetometer

Michael Romalis
Princeton University
Princeton, NJ 08544

We have developed a co-magnetometer consisting of overlapping ensembles of polarized ^{3}He and K atoms for tests of Lorentz violation and other precision measurements. In the device ^{3}He atoms are polarized by spin-exchange with optically-pumped K atoms, and their spin precession is detected through their effect on the spins of K atoms. Using an appropriate combination of magnetic fields, the co-magnetometer response to small changes of external fields can be cancelled while preserving the sensitivity to an anomalous spin coupling that does not scale with the magnetic moments of the atoms. We have demonstrated suppression of external magnetic fields and first-order magnetic-field gradients by a factor of over 1000. The short term sensitivity of the co-magnetometer is determined by the performance of the spin-exchange-relaxation free (SERF) alkali-metal magnetometer and is equal to 2 fT/Hz$^{1/2}$ at 1 Hz. Recently we have been focusing on long-term stability of the co-magnetometer necessary for the Lorentz-violation search. We developed techniques for independently measuring various misalignment parameters and setting them to zero to suppress most spurious effects to second order. We are currently conducting long-term tests of the system and will present the results on the Allan variance.

FLIGHT QUALIFIED SUPERCONDUCTING QUANTUM INTERFERENCE DEVICE (SQUID) CONTROL ELECTRONICS DESIGN STATUS & APPLICATIONS

Kerry L. Neal and Thomas S. Adams

Design_Net Engineering LLC, 10311 W. Hampden Avenue, Suite A-107, Lakewood, Colorado 80227,
Tel: 303-462-0096, Fax: 303-462-0388

ABSTRACT

Long-duration manned interplanetary space flight as envisioned for the exploration of Mars will subject the astronauts to severe environments, not just from the harsh external space environments, but also from the physical and psychological stress of prolonged confinement, weightlessness, and the ever present danger of catastrophic mishap with little hope of assistance or rescue. These conditions could conceivably lead to the psychological and physiological breakdown of one or more crew members, thereby endangering the success of the mission. New technologies need to be developed to help monitor and forecast crew physical and mental health trends as the mission proceeds. One such new technology involves the use of extremely sensitive sensors used to monitor and map human brain activity. These sensors are based on the Super Conducting Quantum Interference Device (SQUID) technology, up until now used primarily in low temperature physics applications. However, SQUID-based sensors have also been demonstrated to be sensitive enough to monitor and map brain activity. To date, this technology has been demonstrated using ground-based commercially available SQUID Control Electronics (SCE), but in order to propose this technology for manned space flight, a system including the electronics must be developed that can operate reliably within a manned spacecraft environment. Just such a "flight qualified" design has been developed by Design_Net Engineering (DNET) under contract to JPL for the Low Temperature Microgravity Physics Facility (LTMPF) slated to be deployed on the International Space Station. This rad-hard space qualified design has been carried to a level of maturity such that engineering development systems have been provided to the LTMPF PI's and demonstrated successfully. Although the LTMPF SCE is designed to support Low Temperature Physics Experiments on orbit, there is no reason to believe that, with some additional development, it could not function equally well in the application of monitoring the health of Mars bound astronauts.

1. INTRODUCTION

The increasing interest in space flight and manned missions has led to the need for the development of supporting medical technologies and techniques to ensure the safety of the crew and to gain a better understanding of the health risks associated with human exploration missions. Another key area of interest relates to how one's performance might be affected during long-duration spaceflight. Critical to understanding the health and performance of the flight crew is the monitoring of the brain. Analyses of the human brain and its processes can provide insights into the astronauts health, behavior and psychological state. Traditionally, the brain's electrical activity has been monitored on Earth by EEG, a fairly invasive technique, a new and more sensitive technique that is noninvasive has arisen with the development of SQUIDs (superconducting quantum interference devices). This technique called MEG (magneto encephalography) observes the brain's electrical currents by measuring the magnetic fields they produce outside of the skull. The strength of the magnetic fields generated by the brain are very small, between 0.1 and 1 pico-Tesla; a SQUID can measure magnetic fields as small as 1 femto-Tesla. Previous work performed by Design_Net Engineering LLC (DNet) has involved the development of flight qualified SQUID control electronics (SCE) for the Low Temperature Micro-gravity Physics Facility (LTMPF) that is to be flown on the International Space Station (ISS). In this case, the flight qualified SQUIDs are to be used to measure cryogenic temperatures and so the control electronics were designed such that the SQUIDs would be sensitive down to sub-nano-Kelvin level temperatures and to have an associated noise of <5 micro-flux quanta (Φ_o) which is equivalent to ~ 5 femto-Tesla/√Hz. This is more than sensitive enough to also be suitable for the aforementioned MEG system to monitor a brain's electrical activity. Thus, it seems a logical and cost effective step would be to utilize the prior successful flight qualified SQUID control electronics design work of DNet in the development of a flight qualified MEG system for use on manned missions. These Represent only two applications for space qualified high reliability SQUID sensor technology. Table 1 below describes these and others.

2. Application Identification & Driving Mission Requirements

- Current Applications for Space Flight Qualified High Reliability SQUID Based Sensors & Readout/Control Electronics:

Application	Resolution	Magnetic Flux Density Equivalent	Flux Equivalent
High Resolution Thermometry			
- Low Temperature Microgravity Physics Facility	**10^{-10} Kelvin**	**5×10^{-15} Tesla**	**5×10^{-6} $\Phi_o/\sqrt{Hz}$**
* Stanford University – Super Conducting Microwave Oscillator (SUMO)			
* University of New Mexico – Critical Dynamics in Microgravity (DYNAMX)			
* Jet Propulsion Lab – Precision Atomic Clock In Space (PARCS)			
* California Institute of Technology–(CQ)			
* Jet Propulsion Lab (MISTE)			

- Other Relevant Space Applications and their example sensor requirements:

Application	Resolution	Magnetic Flux Density Equivalent	Flux Equivalent
Magneto Encephalography		**5×10^{-15} Tesla**	**5×10^{-6} $\Phi_o/\sqrt{Hz}$**
Electro Encephalography			
Gravity Wave Detection			
- Goddard Space Flight Center– Laser Interferometer Space Antenna (LISA)			
* SQUID-based GW sensor	$h \le 10^{-23}$	5×10^{-16} Tesla/√Hz	$\delta\phi = 10^{-7}$ $\phi_o/\sqrt{Hz}$
- Stanford University– LISA Disturbance Reduction System (DRS)			
* SQUID-based accelerometer	$x \le 10^{-9}$ m		
- NASA/ESA – Satellite Test of Equivalence Principle (STEP)			
* Stanford University – SQUID-based accelerometer	$x \le 10^{-15}$ m		

3. SQUID-Based High-Resolution Thermometry

SQUID based high-resolution thermometers (HRT) are now designed to be operable at very high resolutions. These devices are regularly used for low temperature measurements, in particular they are used to study the phase transition of liquid helium e.g. to make high-precision measurements of dynamic properties of liquid helium (^{4}He) as it transitions between a normal and superfluid state.

A SQUID based HRT consists of a superconducting flux tube, a superconducting pick-up loop (flux transformer), a salt pill, a SQUID input coil, a SQUID magnetometer, a heat switch and thermal contact wires. A schematic showing all the key components of a HRT is shown in Figure 1.

The super-conducting flux tube is usually made out of niobium and is used to capture a very stable magnetic field (~100G) as it initially cools down past its superconducting transition temperature. The magnetic field is supplied by a solenoid, which is turned off after the magnetic field has been captured. The salt pill, which consists of a magnetic salt material is located inside the superconducting flux tube and is used as the temperature sensor, since its magnetization changes with temperature. If there is a change in temperature, this will induce a change in magnetization, which will result in a small current flowing in the superconducting pick-up loop. The SQUID and its associated electronics convert this current into a large voltage. Note a heat switch is generally attached to a section of the pick-up loop, since it enables it to be heated above its superconducting temperature when necessary, this is required to set the current in the loop to zero.

The behavior of the superconducting pick-up loop is based upon the law of superconductivity and not Faraday's electromagnetic induction law, specifically, the number of flux quanta, Φ_o, inside a superconducting loop is conserved as long as the loop remains superconductive. The superconducting pick-up loop which surrounds the salt pill is connected to another superconducting coil which resides inside the SQUID sensor package. Therefore this configuration forms a closed superconducting loop and is known as the flux transformer. An illustration of a simple flux transformer that consists of a single-turn loop around a salt pill and an identical one-turn loop in a SQUID sensor package is shown in Figure 2. A photograph of a flight qualified SQUID-based HRT is shown in Figure 3.

As you can see Figure 2 is simplistically illustrating the operating principle of a flux transformer. As mentioned briefly earlier, a temperature change causes the magnetic salt pill to change its magnetization, so in this case assume the temperature changes by an amount which causes the salt pill to add 1 Φ_o inside the closed-loop superconductor. Therefore, it can be seen that in order for the loop to conserve the number of fluxes inside it, it needs to have sufficient current flowing inside its wire so that it produces 1/2 Φ_o in the pick-up loop and 1/2 Φ_o inside the SQUID package. Note the flux generated by the current points in opposite directions to that added in by the salt pill, thus they cancel each other out and the number of flux quanta, Φ_o, inside the superconducting loop is conserved.

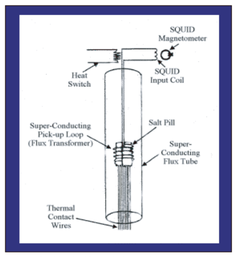

Fig. 1 High-Resolution Thermometer Components

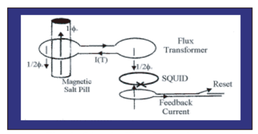

Fig. 2 Simple Flux Transformer

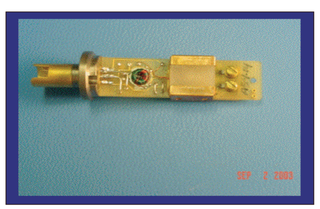

Fig. 3 Flight Qualified SQUID-Based HRT (LTMPF – Quantum Design)

AKNOWLEDGEMENTS

The authors wish to thank Drs. Inseob Hahn and Talso C. P. Chui of the Jet Propulsion Lab, Dr. D. Sergatskov of the University of New Mexico, Dr. John A. Lipa of Stanford University for their invaluable support and advice. The authors also wish to extend gratitude to Drs. Rachel Leach and Kenneth Center of Design_Net Engineering for their invaluable help with the data collection, market research and production of this poster.

For further details regarding the operation and the theory of noise of high-resolution thermometers see *"SQUID-based high-resolution thermometer - Talso C. P. Chui"*.

4. LTMPF

The Low Temperature Microgravity Physics Facility (LTMPF) project is a reusable science facility that will be flown on the International Space Station (ISS). It will be attached to the ISS's Japanese Experiment Module's Exposed Facility (JEM-EF), and is expected to have a 5 mission life cycle. Each mission provides a microgravity platform from which 2 different and independent low temperature physics experiments can be conducted. Each mission is expected to have a minimum lifetime of approximately 4.5 months, 3 months of which are to be dedicated to data acquisition. This type of platform is desired since the presence of a strong gravitational force can ultimately distort experiment measurements and limit the observations that can be made. In the low-gravity environment, scientists will have the unique opportunity to explore and study properties of fundamental physics that can not be observed in earth-based observatories.

The LTMP facility is intended to be a reusable and versatile commodity for future missions/projects. It is a 'class C' project and thus inherently has a lot of single mode faults and failures, but to date there are no plans to protect against these. Specifically, the C classification refers to "an economically, re-flyable or repeatable payload, where the re-flight is planned and where there is no impact of soft failure other than the cost of repair and re-flight". The low temperature micro-gravity physics facility dewar assembly is shown in Figure 4.

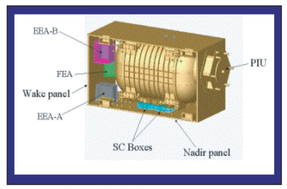

Fig. 4 LTMPF Dewar Assembly

To date, eight experiments have been identified to take advantage of the LTMP facility, namely; the Critical Dynamics in Microgravity Experiment (DYNAMX/CQ), the Microgravity Scaling Theory Experiment (MISTE/COEX), the Superfluid Universality Experiment (SUE), the Experiments Along Coexistance Near Tricriticality (EXACT), the Boundary Effects Near the Superfluid Transition (BEST), the Superconducting Microwave Oscillator project (SUMO), the Kinetics of the Superfluid Helium Phase Transition (KISHT), and the Superfluid Hydrodynamics Experiment (SHE). Currently, the DYNAMX and SUMO experiments have been selected to be the first pair of experiment candidates to make use of the LTMP facility, on the M1 mission. Figures 5 & 6 show schematics of the configuration for an example experiment.

The main types of thermometry instrumentation that will be used on M1 comprise of Germanium Resistance Thermometers (GRTs) and Superconducting Quantum Interference Device (SQUID) based High Resolution Thermometers (HRTs). In the narrow temperature range the GRTs have a sensitivity of the order of ~10kOhm/K. HRTs have a sensitivity on the order of 1 to 10 Φ_o per μK. Where Φ_o = magnetic flux quanta ≈ 2×10^{-15} Weber.

Fig. 5 DYNAMX Experiment Configuration

Fig. 6 SUMO Experiment Configuration

5. LTMPF Electronics & Software Subsystem (ESS)

The role of the Electronics & Software Subsystem (ESS) is to provide the LTMPF with communication and control functionality, as such it comprises:

- Electronics Assemblies - 2 experiment, 1 facility, 2 SQUID plus other miscellaneous adaptor boxes
- Facility software - including internal & external communications
- Cabling

The Electronics and Software developed for this program will provide the electrical and software interfaces for the facility to the JEM-EF through the PIU. Electrical power is provided on a single 120 volt circuit which is protected and switched by the ISS. Internally, the facility must provide additional circuit protection and switching. The command interface is via 1553B where the LTMPF is a Remote Terminal (RT) with one RT address. Some housekeeping telemetry is returned to the ISS via the 1553B interface for the purpose of crew monitoring to determine the basic health of the facility. The primary telemetry downlink for science is via a 10 Mbps Ethernet interface (IEEE 802.3, 10-Base-T) in which telemetry data from the LTMPF is sent from a single IP address to the ISS for downlink. The Electronics and Software must provide command, control, data acquisition, and telemetry services for the science instruments as well as for the cryostat.

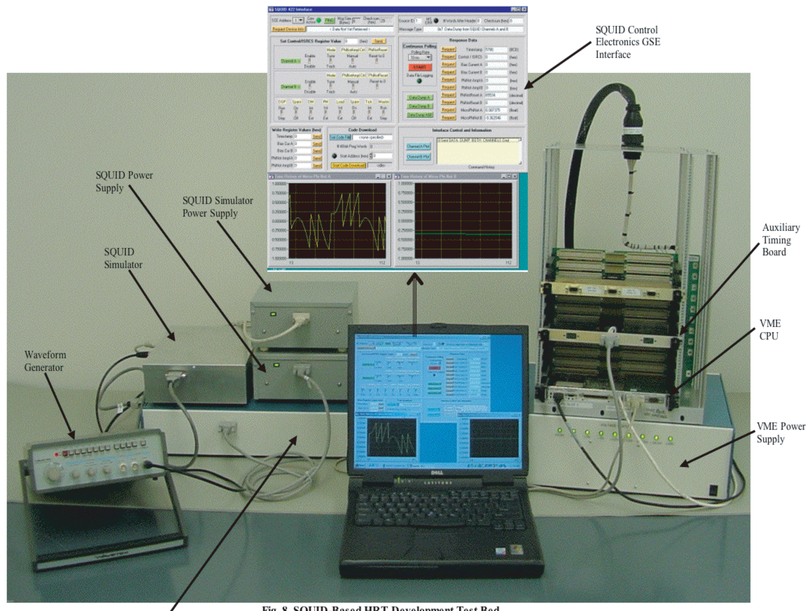

Fig. 8 SQUID-Based HRT Development Test Bed

The primary science measurements provided by the facility are the Germanium Resistance Thermometer (GRT) and High Resolution Thermometer (HRT) temperatures. In addition, the facility must provide Low and High Precision Heater drivers (LPH & HPH). Other precision science measurements may be required and support must be provided for these experiment unique capabilities. Figure 7 illustrates the block diagram of the entire ESS. It shows its interrelationship of the various components and how the signals connect to external and internal interfaces. Figures 10, 11 & 12 show photographs of some of the LTMPF ESS assemblies.

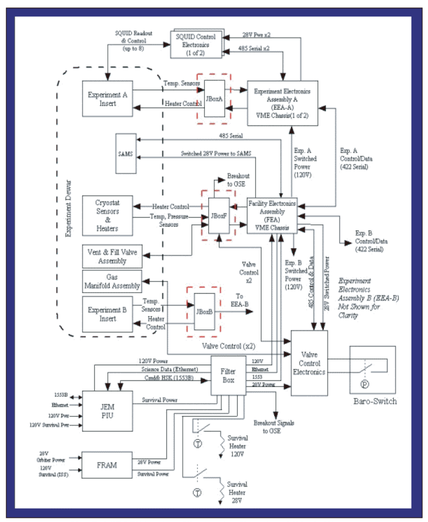

Fig. 7 LTMPF System Electronics Functional Block Diagram

6. SQUID Control Electronics (SCE)

The role of the SQUID Control Electronics (SCE) is to provide the SQUID hardware with communication and control functionality, as such it comprises:

- Power converter board
- DSP controller board
- Pre-amp board
- SCE software

Specifically, the SCE shall use a DSP based SQUID controller system with code that is downloaded from the associated VME chassis. The SCE boards shall each control up to 4 SQUIDS and shall be stackable for convenience in packaging and sparing. The SCEs will be provided with switched 28V power from the corresponding EEA VME chassis which will also monitor their power consumption. The communication interface shall be a simple serial protocol which will allow a modified PC to act as the SCE GSE. The SCE has an electronic circuitry known as the *SQUID Controller*, which detects changes in the flux contribution from the SQUID input coil. Note the electronics can measure changes in the flux contribution from the input coil that are very much smaller than a flux quantum Φ_o. This is true because a SQUID biased to where $\partial V/\partial\Phi$ is maximized produces a considerable output voltage _V in response to a small input flux _Φ. In addition to the bias and modulation signals, the SQUID Controller also provides a feedback signal for the purpose of achieving *flux lock*. To achieve this, the SQUID Controller measures the AC voltage across the SQUID and provides a detected output, which (by means of a control algorithm) is fed back to the SQUID in such a way as to minimize (or ideally, to null) the AC voltage across the SQUID. Figures 8 & 9 show photographs of the SQUID-Based HRT Development Testbed and the SCE development board, respectively. Note the flight version of the SCE board will be significantly smaller than the development board.

6.1 SCE Software

There are two means by which interactions with the SCE may be accomplished. During initial development, a PC host (GSE) interface was created to facilitate the sending of commands to the DSP and the collection of data using consecutive polls of the channel data registers. This environment was developed in National Instrument's LabWindows/CVI (C for Virtual Instrumentation). This GUI provides a means by which all functionality of the DSP can be accessed and tested. It was used extensively during the hardware development phase and can still be used as a stand-along laboratory tool to control the electronics. As part of the LTMPF flight software development effort, modules have been written to facilitate control of the SCE through PowerPC resident RS-422 serial drivers. In the flight implementation, a VME timing board distributes the 16MHz clock signal to the DSP. This timing signal is also distributed on the VME backplane so that the FPGAs of all instrument boards resident in the chassis are kept in synchronous operation. This timing board also generates a master interrupt at 10ms intervals, so that the CPU can signal hardware driver tasks to collect instrument data on published boundaries. The SCE raw data, consisting of Resets and MicroPhiNaught (Φ_o), are stored in arrays, formed into coherent telemetry packets on one-second boundaries, and streamed out of the CPU over Ethernet. The TReK software suite, developed at Marshal Space Flight Center, is used for acquisition and archiving of the telemetry stream. LabView Vis, created by DNet, retrieve data packets from the TReK telemetry database and display them in real-time for data monitoring purposes. Configuration of the SCE in the flight software is accomplished by sending flight command messages from a LabWindows/CVI chassis command interface to a command server process on the real-time target. This server routes the message to the appropriate SCE driver task, which processes the request by engaging in a command/response communication sequence with the SCE DSP.

6.2 SCE Requirements

The SCE design has the following capabilities to support the LTMPF experiment requirements:

- Operates a Quantum Design dc SQUID (QD50):
  - Provides proper 'modulation', 'feedback' and 'bias' signals
  - Provides transformer-coupling and receives 'signal' output
- Meets the following system performance requirements:
  - Contributes less than 30 $\mu\Phi_o/Hz^{0.5}$
  - Maintains count for rates up to 1000 resets/sec
  - Provides stability better than 20 $\mu\Phi_o$/1000 seconds over the operating temperature and voltage ranges of SQUID Control Electronics
- Maintains flux lock and keeps count of resets over operating range (>100000 Φ_o):
  - Keeps dynamic range of the 'feedback' signal < $2\Phi_o$.
  - Permits the operator to set bias current, modulation amplitude, and output gain as well as reset the Flux-lock Loop and to open the loop.
  - Provides as its output a measurement of flux integrating the number of resets from a calibration point and a fractional portion.

6.3 SQUID Simulator

A SQUID simulator was also designed and built to support the needs of the SCE design work. The SQUID simulator is a very valuable development tool as it eliminates the need for a real SQUID and thus the associated liquid Helium, saving time and simplifying the development test setup. This approach is also advantageous because it removes the need to expose the relatively expensive and sensitive SQUID sensors to the potentially harmful development environment.

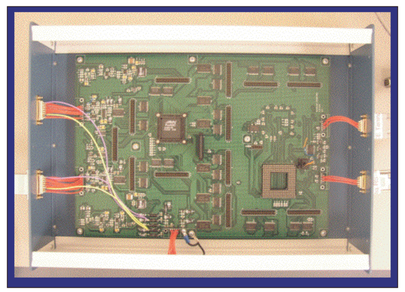

Fig. 8 LTMPF ESS SCE Development Board
(Flight version will be significantly smaller)

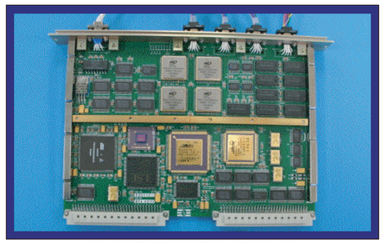

Fig. 9 LTMPF ESS Flight CPU Board
(SEAKR Eng. under contract to DNet)

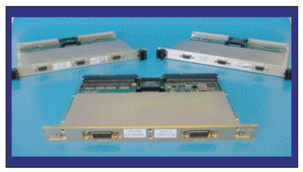

Fig. 10 LTMPF ESS VME EM Boards (GRT, HPH, LPH)

Fig. 11 LTMPF ESS VME Chassis with Boards

Status of the SUMO experiment

John Lipa
Stanford University, Physics Department
Stanford, CA 94305

We describe the present status of the SUMO experiment and consider some alternative flight scenarios.

Theoretical Investigations of Near-Critical Superfluid Dynamics

Peter Weichman
ALPHATECH, Inc.
6 New England Executive Park
Burlington, MA 01803

I will discuss recent as well as proposed research in the area of superfluid dynamics close to the lambda point, with special emphasis on nonequilibrium interface states in which a combination of gravity and applied heat current supports coexistence of superfluid and normal phases, with a well defined interface between them. Various calculations aimed at understanding the steady state structure of these interfaces, as well as their near-steady-state dynamics under the influence of various external perturbations, such second sound and vibration, will be described. I will also describe recent and planned investigations of the so-called self-organized critical (SOC) state, which supports a finite temperature gradient in the superfluid phase by generating a steady flux of vortex rings expanding across the direction of heat flow. Of interest are the fluctuations and spatial correlations in this state, its associated nonequilibrium specific heat, and the effects of a superfluid-SOC interface on the measurement of the heat capacity at constant heat current.
Reference: P. B. Weichman, A. W. Harter and D. L. Goodstein, Rev. Mod. Phys. Vol. **73**, pp. 1-16 (2001).

Superfluid Transitions in Bosonic Atom-Molecule Mixtures Near Feshbach Resonance

Peter Weichman
ALPHATECH, Inc.
6 New England Executive Park
Burlington, MA 01803

I will describe theoretical studies of bosonic atoms near a Feshbach resonance, where we predict that in addition to standard normal and atomic superfluid phases, the system generically exhibits a distinct phase of matter: a molecular superfluid, where molecules are superfluid while atoms are not. The zero- and finite-temperature properties of the molecular superfluid (a bosonic, strong coupling analog of a BCS superconductor), and the quantum and classical phase transitions between the normal, molecular superfluid and atomic superfluid states will be described. Reference: L. Radzihovsky, J. Park and P. B. Weichman http://xxx.arxiv.cornell.edu/abs/cond-mat/0312237 (Phys. Rev. Lett., in press, 2004).